

Bloch Structures in a Rotating Bose-Einstein Condensate

Hiroki Saito and Masahito Ueda

*Department of Physics, Tokyo Institute of Technology, Tokyo 152-8551, Japan
and CREST, Japan Science and Technology Corporation (JST), Saitama 332-0012, Japan*

(Dated: February 8, 2020)

A rotating Bose-Einstein condensate is shown to exhibit a Bloch band structure without the need of periodic potential. Vortices enter the condensate by a mechanism similar to the Bragg reflection, if the frequency of a rotating drive or the strength of interaction is adiabatically changed. A localized state analogous to a gap soliton in a periodic system is predicted near the edge of the Brillouin zone.

The Bloch band is crucial to our understanding of the behaviors of periodic systems, such as electronic states in solids [1], atom dynamics in optical lattices [2], and Cooper-pair tunneling in small Josephson junctions [3]. The underlying physics common to all of these is the Bragg reflection that occurs at the edges of the Brillouin zone. The resultant Bloch band leads to various interesting phenomena, such as Bloch oscillations [1] (a particle in a periodic potential driven by a weak constant force cannot be accelerated indefinitely but oscillates in real space) and formation of gap solitons [4] (localized wave packets arising from the balance between negative-mass dispersion and repulsive interaction); both phenomena have recently been observed with a Bose-Einstein condensate (BEC) in an optical lattice [5, 6].

In this Letter, we show that yet another system — a BEC confined in a rotating harmonic-plus-quartic potential — exhibits a Bloch band structure, and investigate the associated novel phenomena. Seemingly this system has no periodic structure, but may be considered to be a quasi-1D periodic system in the following sense. When the rotating frequency of the potential is high, the quartic potential $\propto r^4$, together with the centrifugal one $\propto -r^2$, produces a Mexican-hat shaped potential [7] whose minima form a quasi-1D toroidal geometry. Under such circumstances any perturbation $V(\theta)$ that is needed to drive the system into rotation by breaking the axisymmetry of the potential serves as a “periodic” potential since $V(\theta) = V(\theta + 2\pi)$, where θ denotes the azimuthal angle.

In the present system, we will show that the Bragg reflection causes vortex nucleation. Since this process occurs adiabatically, in contrast to a method invoking dynamical instabilities [8, 9], we can obtain the vortex states without heating the atomic cloud. A stirring technique to produce vortices without heating has also been proposed in Refs. [10, 11]. Another scheme that adiabatically nucleates vortices is based on phase engineering techniques [12, 13, 14]. We will also show that a localized state is generated even with repulsive interactions, which is analogous to gap solitons in periodic systems [4].

We begin by discussing a BEC in a 1D ring to understand the essence of the phenomena. We assume that a rotating potential takes the form $V(\theta, t) = \varepsilon \cos n(\theta - \Omega t)$.

In a frame rotating at frequency Ω , the potential V becomes time-independent, and the Gross-Pitaevskii (GP) equation is given by

$$\left(-\frac{\partial^2}{\partial \theta^2} + i\Omega \frac{\partial}{\partial \theta} + \varepsilon \cos n\theta + \gamma |\psi_{1D}|^2\right) \psi_{1D} = \mu \psi_{1D}, \quad (1)$$

where energy and time are measured in units of $\hbar^2/(2mR^2)$ and $2mR^2/\hbar$ with m and R being the atomic mass and the radius of the ring. The wave function is normalized as $\int_0^{2\pi} |\psi_{1D}|^2 d\theta = 1$, and γ characterizes the strength of interaction.

First, let us consider the noninteracting case ($\gamma = 0$). Introducing a new variable $\phi \equiv e^{-i\Omega\theta/2} \psi_{1D}$, we transform Eq. (1) into the Mathieu equation $(-\partial_\theta^2 + \varepsilon \cos n\theta)\phi = E\phi$, where $E \equiv \mu + \Omega^2/4$ plays the role of the “total energy” in our Bloch band picture. Then the solution satisfies $\phi(\theta + \Theta_0) = e^{i(p-\Omega/2)\Theta_0} \phi(\theta)$, with $\Theta_0 \equiv 2\pi/n$ being the period of the potential V , and p an integer. It follows that $p - \Omega/2$ may be regarded as the quasimomentum, indicating that we can move in the quasimomentum space by changing Ω . Since the unit “reciprocal lattice vector” is $2\pi/\Theta_0 = n$, the Bragg reflection occurs only between the states whose angular momenta differ by $n, 2n, \dots$ (Bragg’s law). Consequently there are n independent branches corresponding to $p = 0, \dots, n-1$ modulo n . Figure 1 shows E and the angular momentum $\langle L \rangle = -i \int_0^{2\pi} \psi_{1D}^* \partial_\theta \psi_{1D} d\theta$ as functions of Ω for the first and second Bloch bands with $n = 2$ and $\varepsilon = 0.1$. Two independent branches exist in this case, and are distinguished by the solid and dotted curves. The Bloch band structure in Fig. 1 indicates that if we adiabatically increase or decrease Ω across $\Omega = 2$, the nonvortex state $\psi_{1D} \simeq 1/\sqrt{2\pi}$ transforms to the vortex state $\psi_{1D} \simeq e^{2i\theta}/\sqrt{2\pi}$, and vice versa. The time scale of the adiabatic change must be much longer than the inverse energy gap $\simeq \varepsilon^{-1}$.

When $|\gamma| \gtrsim \varepsilon$, the system exhibits hysteretic behavior, and a loop structure emerges in the Bloch bands [15] as shown in Fig. 1. We see that the first (second) band forms a loop for $\gamma = 1(-1)$; then the adiabatic nucleation of vortices is not possible with increasing (decreasing) Ω because the nonlinear Landau-Zener transition [15] occurs no matter how slow the change of Ω . It can be shown that the states on the loop have dynam-

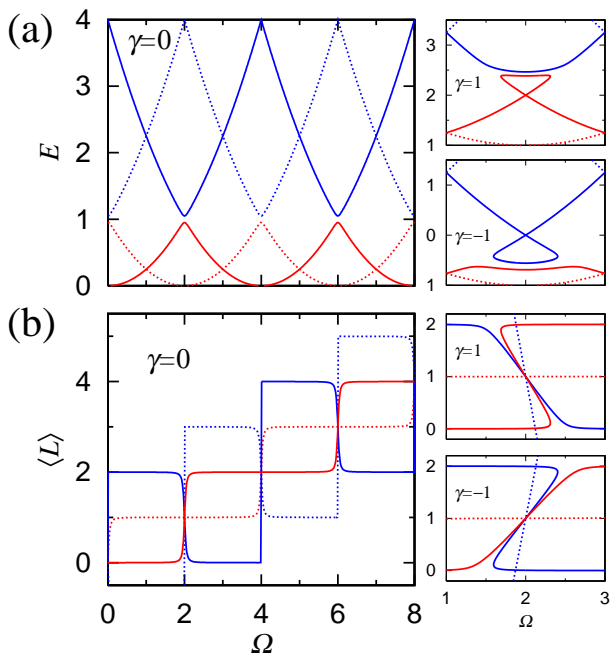


FIG. 1: (a) $E \equiv \mu + \Omega^2/4$ and (b) $\langle L \rangle \equiv -i \int \psi_{1D}^* \partial_\theta \psi_{1D} d\theta$ of the first (red curves) and the second (blue curves) Bloch bands for the noninteracting (main panels) and interacting (right panels) BECs in a 1D ring described by Eq. (1) with $V(\theta) = 0.1 \cos 2\theta$. The solid and dotted curves refer to two independent branches.

ical instability that breaks the symmetry of the system $|\psi_{1D}(\theta)| = |\psi_{1D}(\theta + \Theta_0)|$. This instability is similar to the one that forms gap solitons in a BEC in an optical lattice [16].

We now consider a BEC in a harmonic-plus-quartic potential with a rotating stirrer. We assume that the axial trapping energy $\hbar\omega_z$ is much larger than the other characteristic energies (a tight pancake-shaped trap) so that the system is effectively 2D. The external potential in the corotating frame of reference takes the form $V(\mathbf{r}) = r^2/2 + Kr^4/4 + \varepsilon r^2 \cos 2\theta$, where K is a constant and the third term $\varepsilon(x^2 - y^2)$ is a stirring potential which can be produced by laser beams propagating in the z direction. Such an anharmonic potential was theoretically considered in Refs. [7, 17, 18] and has recently been realized experimentally [19]. We normalize the length, time, energy, and wave function by $d_0 \equiv (\hbar/m\omega_\perp)$, ω_\perp^{-1} , $\hbar\omega_\perp$, and \sqrt{N}/d_0 , respectively, with ω_\perp and N being the frequency of the radial harmonic trap and the number of atoms. The wave function is then normalized as $\int |\psi_{2D}|^2 d\mathbf{r} = 1$. The time-dependent GP equation in the frame corotating with the stirring potential at frequency Ω is given by

$$i \frac{\partial \psi_{2D}}{\partial t} = \left(-\frac{1}{2} \nabla^2 + i\Omega \frac{\partial}{\partial \theta} + V(\mathbf{r}) + g|\psi_{2D}|^2 \right) \psi_{2D}, \quad (2)$$

where $g = [\omega_z/(2\pi\omega_\perp)]^{1/2} 4\pi N a/d_0$ characterizes an ef-

fective strength of interaction in 2D [20] with a being the s-wave scattering length.

When $\Omega \gg 1$, the system described by Eq. (2) can be approximated by a quasi-1D ring [7]. Assuming $\psi_{2D} \simeq f(r)e^{i\ell\theta}/\sqrt{2\pi}$, we find that an effective potential for the radial wave function is given by $\ell^2/(2r^2) + r^2/2 + Kr^4/4$. This potential has a minimum at $r \simeq (\ell^2/K)^{1/6}$ for $\ell \gg 1$, and the effective frequency around it is $\omega_{\text{eff}} \simeq \sqrt{6}(\ell K)^{1/3}$. If ω_{eff} is much larger than other characteristic frequencies, the dynamics of $f(r)$ can be ignored. After normalization of the time by $\rho^{-2} \equiv \int r|f|^2 r^{-2} dr$, the equation of motion for θ reduces to Eq. (1), where γ is given by $2g\rho^2 \int r|f|^4 dr$. Thus, the system described by Eq. (2) exhibits the quasi-1D circular flow for large angular momentum [7], and we expect that a Bloch band structure emerges. We show below that this is true even for $\Omega \sim 1$ and $\ell \sim 1$.

Figure 2 (a) shows the angular momentum $\langle L \rangle = -i \int \psi_{2D}^* \partial_\theta \psi_{2D} d\mathbf{r}$ and the density and phase profiles (insets) of the noninteracting stationary states of Eq. (2) [21]. We find that the behavior of $\langle L \rangle$ is similar to that in Fig. 1 (b). When we start from the ground state with $\langle L \rangle = 0$ (1-1), two vortices enter at $\Omega \simeq 1.57$ (1-2), producing a doubly-quantized vortex (1-3) [17]. Increasing the rotation frequency Ω further, we can nucleate two more vortices in the condensate [(1-4) and (1-5)]. If we follow the branch starting from $\langle L \rangle = 2$ (2-1), the two vortices escape out of the condensate with *increasing* Ω [(2-2) and (2-3)], and then four vortices enter at $\Omega \simeq 1.7$ (2-4). It should be noted that the Bloch band picture holds even for the nonrotating gas, while the ring-shaped profile manifests itself only if the gas is rotating [cf. (1-1) and (2-3)].

The frequencies at which the Bragg reflection occurs in Fig. 2 (a) are different from those in Fig. 1. The difference arises from the dispersion relation of the vortex states in 2D, i.e., the relation between the energy and angular momentum. In the 1D case, the energy is given by $E_m^{1D} = \int [q\psi_m^{1D*}(-\partial_\theta^2 + i\Omega\partial_\theta)\psi_m^{1D} + \gamma|\psi_m^{1D}|^4/2] d\theta = m^2 - \Omega m + \gamma/(4\pi)$ for $\psi_m^{1D} = e^{im\theta}/\sqrt{2\pi}$. The Bragg reflection between ψ_m^{1D} and ψ_{m+2}^{1D} occurs when $E_m^{1D} = E_{m+2}^{1D}$, i.e., $\Omega = 2m + 2$. In the 2D case, we employ a variational wave function $\psi_m^{2D} = (\pi|m|!)^{-1/2} d_m^{-|m|-1} r^{|m|} \exp[-r^2/(2d_m^2) + im\theta]$ to obtain $E_m^{2D} = (|m|+1)(d_m^{-2} + d_m^2)/2 + K(|m|+1)(|m|+2)d_m^4/4 - \Omega m + g(2|m|)!/[2^{2|m|+2}\pi|m|^2 d_m^2]$, where the variational parameter d_m is determined from $\partial E_m^{2D}/\partial d_m = 0$. When $K = 1$ and $g = 0$, the condition for Bragg reflections to occur between ψ_m^{2D} and ψ_{m+2}^{2D} ($E_m^{2D} = E_{m+2}^{2D}$) for $m = 0, 2, \text{ and } 4$ is satisfied at $\Omega = 1.58, 1.83, \text{ and } 2.03$, respectively, which are in good agreement with the numerical results in Fig. 2 (a) (corresponding to the points at which the red and blue curves cross with $\langle L \rangle$ changing by ± 2).

The energy gap can also be obtained by a variational method. The matrix element of the stirring potential,

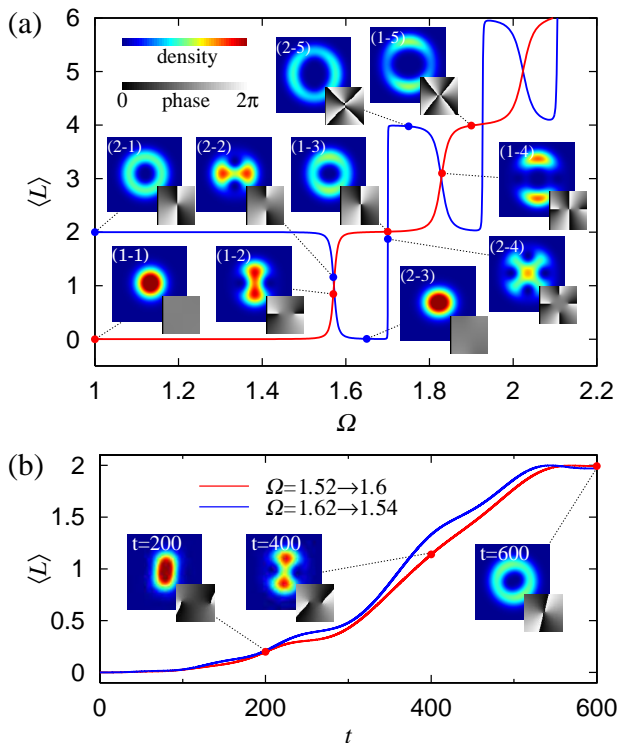


FIG. 2: (a) Angular momentum $\langle L \rangle$ versus rotation frequency Ω of the stationary states of the GP equation (2) with $g = 0$, $K = 1$, and $\varepsilon = 0.02$. The images (1-1)-(1-5) [(2-1)-(2-5)] correspond to the branch indicated by the red (blue) curve. (b) Time evolutions with $\lambda = 0.03$, where Ω is linearly changed from 1.52 to 1.6 (red curve) and from 1.62 to 1.54 (blue curve) during $0 \leq t \leq 600$. The initial state is the ground state, and ε is linearly ramped up from 0 to 0.04 during $0 \leq t \leq 200$, kept at 0.04 during $200 \leq t \leq 400$, and ramped down from 0.04 to 0 during $400 \leq t \leq 600$ to suppress nonadiabatic disturbances. The size of the images is 5×5 in units of $(\hbar/m\omega_{\perp})^{1/2}$.

for example, between ψ_0^{2D} and ψ_2^{2D} is calculated to be $|\int \psi_2^{2D*} \psi_0^{2D} \varepsilon r^2 \cos 2\theta d\mathbf{r}| \simeq 0.46\varepsilon$ for $K = 1$. The energy gap at $\Omega \simeq 1.57$ is then given by $\simeq 0.92\varepsilon$, which also agrees very well with the numerical result $\simeq 0.91\varepsilon$.

The Bloch band structure in Fig. 2 (a) indicates that if we prepare the nonvortex state at $\Omega \lesssim 1.55$, and adiabatically increase Ω to above $\Omega \simeq 1.6$, we obtain a doubly-quantized vortex state by following the red curve. Interestingly, we can nucleate vortices also by *decreasing* Ω , that is, by preparing a nonvortex state for $1.6 \lesssim \Omega \lesssim 1.7$ and decreasing Ω to below $\Omega \simeq 1.55$ by following the second Bloch band (blue curve). Figure 2 (b) illustrates these adiabatic processes. In order to examine the effect of dissipation on the adiabatic processes, we replace i with $i + \lambda$ on the left-hand side of Eq. (2), where a constant λ is taken to be 0.03 [22]. We prepare the nonvortex ground state with $g = 0$, and gradually ramp up Ω from 1.52 to 1.6 [red curve in Fig. 2 (b)], or ramp it down from 1.62 to 1.54 (blue curve). As expected, two density holes with phase singularities come from infinity,

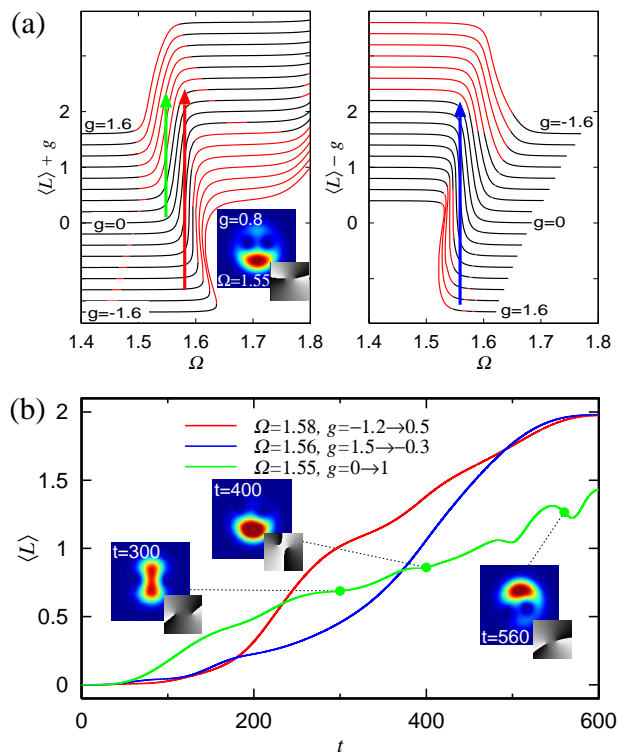


FIG. 3: (a) The g dependence of the first and second bands (left and right panels) with $K = 1$ and $\varepsilon = 0.02$, where the curves are offset by $\pm g$ for clarity. The dynamically unstable regions are indicated by the red curves. The inset shows a localized stationary state –“gap soliton”– formed near the first band at $g = 0.8$ and $\Omega = 1.55$. (b) Time evolutions with $\lambda = 0.03$ and $K = 1$, where g is linearly ramped from -1.2 to 0.5 with $\Omega = 1.58$ [red curve, corresponding to the red arrow in (a)], from 1.5 to -0.3 with $\Omega = 1.56$ (blue curve, blue arrow), and from 0 to 1 with $\Omega = 1.55$ (green curve, green arrow). A small perturbation to break the axisymmetry is added to the initial state. The change of ε in the red and blue curves is the same as in Fig. 2 (b), and $\varepsilon = 0.04$ is kept during $200 \leq t \leq 600$ in the green curve.

and unite to form a doubly-quantized vortex. We note that the behaviors in Fig. 2 (b) are almost the same as for the dissipation-free case ($\lambda = 0$), indicating that the process is robust against dissipation. The energy gap between the first and second Bloch bands at $\Omega \simeq 1.57$ is $\simeq 0.036$ for $\varepsilon = 0.04$. According to the Landau-Zener formula, the transition probability between the energy gap, i.e., the probability that the nonvortex state remains so, is below 1% in the situation in Fig. 2 (b), in agreement with our numerical result.

In the case of $g \neq 0$, the interaction bends the Bloch bands as shown in Fig. 3 (a), yielding hysteresis as in the 1D case. We note that the region of Ω in which the Bragg reflection occurs is shifted due to the interaction. The shift is attributed to the difference in interaction energies between the nonvortex and vortex states. To show this we again employ the variational wave function ψ_m^{2D} . We

find that the condition for the Bragg reflection to occur between ψ_0^{2D} and ψ_2^{2D} , i.e., $E_0^{2D} = E_2^{2D}$, is satisfied at $\Omega = 1.53$ for $g = 1.6$ and $\Omega = 1.64$ for $g = -1.6$, in qualitative agreement with the shifts shown in Fig. 3 (a). Since the interaction term of E_m^{1D} is independent of m , the shift does not occur in 1D (see Fig. 1).

The shift in the position of the Bragg reflection implies the possibility of the adiabatic nucleation of vortices by changing the strength of interaction using, e.g., the Feshbach resonance [23], at fixed Ω . For example, at $\Omega \simeq 1.58$, the first Bloch band has angular momentum $\langle L \rangle \simeq 0$ for $g \lesssim -1$ [left panel in Fig. 3 (a)], which continuously increases to $\langle L \rangle \simeq 2$ with an increase in the interaction to repulsive (red arrow). Similarly, there is a region in which $\langle L \rangle$ changes from 0 to 2 as g decreases from positive to negative [blue arrow in the right panel in Fig. 3 (a)]. No dynamical instability is present on the red and blue arrows. Figure 3 (b) illustrates these results, where the initial state is the nonvortex ground state, and the strength of interaction is gradually changed with Ω held fixed (red and blue curves). We find that the two vortices are nucleated in a manner similar to that in Fig. 2 (b). The repulsive-to-attractive case is particularly interesting because the attractive interaction is usually considered to hinder vortex nucleation [18].

The adiabatic theorem breaks down when the path enters the region of dynamical instability. A notable example is shown as the green arrow in Fig. 3 (a). For $g \gtrsim 0.6$ at $\Omega \simeq 1.55$, a twofold symmetric state [like the inset (1-2) of Fig. 2 (a)] becomes dynamically unstable against localization into the state shown in the inset of Fig. 3 (a). This localization is due to the interplay between repulsive interaction and negative-mass dispersion around the edge of the Brillouin zone. The localized state can therefore be regarded as an analog of the gap soliton in a periodic system [4]. The green curve in Fig. 3 (b) demonstrates the time evolution corresponding to the path shown as the green arrow in Fig. 3 (a). The twofold symmetry as shown by the inset at $t = 300$ is broken in the course of vortex nucleation, giving rise to two localized states as shown by the insets at $t = 400$ and $t = 560$.

Figure 3 (a) shows that a doubly-quantized vortex state with $\langle L \rangle \simeq 2$ is dynamically unstable (stable) in most of the region with $g < 0$ ($g > 0$). This instability also gives rise to a localized state that undergoes center-of-mass rotation. We find from the numerical analysis that a doubly-quantized vortex state with $g < 0$ evolves into the localized state, followed by the oscillation between these two states in a manner similar to the split-merge oscillations reported in Ref. [24].

In conclusion, we have shown that the Bloch band structure arises in a BEC confined in a harmonic-plus-quartic potential with a rotating drive, which enables us to nucleate vortices adiabatically. The physical mechanism of the vortex nucleation is very similar to the Bragg

reflection at the edge of the Brillouin zone. Interestingly, we can nucleate vortices not only by increasing the stirring frequency but also by decreasing it, or by changing the strength of interaction at a fixed stirring frequency, which may be called a ‘‘Feshbach-induced Bragg reflection’’. The adiabatic processes are robust against dissipation due, e.g., to a thermal cloud. Spontaneous localization of the rotating cloud is predicted, which signals the existence of a gap soliton.

This work was supported by the Special Coordination Funds for Promoting Science and Technology, a 21st Century COE program at Tokyo Tech ‘‘Nanometer-Scale Quantum Physics’’, and a Grant-in-Aid for Scientific Research (Grant No. 15340129) from the Ministry of Education, Science, Sports, and Culture of Japan.

-
- [1] J. M. Ziman, *Theory of Solids* (Cambridge, New York, 1972).
 - [2] For review see P. S. Jessen and I. H. Deutsch, *Adv. At. Mol. Opt. Phys.* **37**, 95 (1996).
 - [3] K. K. Likharev and A. B. Zorin, *J. Low Temp. Phys.* **59**, 347 (1985).
 - [4] P. Meystre, *Atom Optics* (Springer-Verlag, New York, 2001), and references therein.
 - [5] O. Morsch *et al.*, *Phys. Rev. Lett.* **87**, 140402 (2001).
 - [6] B. Eiermann *et al.*, *cond-mat/0402178*.
 - [7] K. Kasamatsu *et al.*, *Phys. Rev. A* **66**, 053606 (2002).
 - [8] S. Sinha and Y. Castin, *Phys. Rev. Lett.* **87**, 190402 (2001).
 - [9] K. W. Madison *et al.*, *Phys. Rev. Lett.* **86**, 4443 (2001).
 - [10] B. Damski *et al.*, *J. Phys. B* **35**, 4051 (2002).
 - [11] B. M. Caradoc-Davies *et al.*, *Phys. Rev. Lett.* **83**, 895 (1999).
 - [12] R. Dum *et al.*, *Phys. Rev. Lett.* **80**, 2972 (1998).
 - [13] J. E. Williams and M. J. Holland, *Nature (London)* **401**, 568 (1999); M. R. Matthews *et al.*, *Phys. Rev. Lett.* **83**, 2498 (1999).
 - [14] M. Nakahara *et al.*, *Physica B* **284-288**, 17 (2000); A. E. Leanhardt *et al.*, *Phys. Rev. Lett.* **89**, 190403 (2002).
 - [15] B. Wu and Q. Niu, *Phys. Rev. A* **61**, 023402 (2000).
 - [16] V. V. Konotop and M. Salerno, *Phys. Rev. A* **65**, 021602(R) (2002).
 - [17] E. Lundh, *Phys. Rev. A* **65**, 043604 (2002).
 - [18] The fact that a vortex can exist in a BEC with weak attractive interactions is also pointed out in E. Lundh *et al.*, *Phys. Rev. Lett.* **92**, 070401 (2004).
 - [19] V. Bretin *et al.*, *Phys. Rev. Lett.* **92**, 050403 (2004).
 - [20] Y. Castin and R. Dum, *Eur. Phys. J. D* **7**, 399 (1999).
 - [21] Here vortices are defined as localized density depletions that have phase singularities. The core size of a vortex is kept from diverging in the limit of $g = 0$ due to the presence of a trapping potential.
 - [22] S. Choi *et al.*, *Phys. Rev. A* **57**, 4057 (1998).
 - [23] S. Inouye *et al.*, *Nature (London)* **392**, 151 (1998).
 - [24] H. Saito and M. Ueda, *Phys. Rev. Lett.* **89**, 190402 (2002); *Phys. Rev. A* **69**, 013604 (2004).